CMLS, Cell. Mol. Life Sci. 56 (1999) 660–669
1420-682X/99/080660-10 $ 1.50 + 0.20/0

CMLS Cellular and Molecular Life Sciences

Review

Three for T: molecular analysis of the low voltage-activated calcium channel family

E. Perez-Reyes

Department of Physiology, Loyola University Medical Center, Maywood (Illinois 60153, USA),
Fax + 1 708 216 6308, e-mail: eperez@luc.edu
Department of Pharmacology, University of Virginia, Charlottesville (Virginia, 22908, USA),
Fax + 1 804 982 3878, e-mail: eperez@virginia.edu

Received 12 May 1999; received after revision 12 July 1999; accepted 14 July 1999

Abstract. Despite the wealth of information on voltage-gated calcium channels, little is known about low voltage-activated, T-type channels. The ability of the antihypertensive drug mibefradil to selectively block T-type channels has generated much interest in their structure, physiology and pharmacology. This review covers the cloning of a new family of calcium channels, their putative structure, the electrophysiological evidence that demonstrated that these complementary DNAs encoded low voltage-activated, T-type channels, the tissue expression of these genes, and concludes with a discussion of their possible physiological roles.

Key words. Calcium channels; molecular cloning; gene expression; antihypertensives; antiepileptics.

Introduction

Early classification schemes separated calcium channels into two broad classes: low voltage-activated (LVA) channels, which open after small depolarizations of a well-polarized membrane (− 80 mV), and high voltage-activated (HVA) channels, which require larger depolarizations. Much is already known about the subunit structure of HVA channels, and there are several reviews on the subject [1–3]. Biochemical, molecular cloning and coexpression studies have established that there are six $\alpha 1$ subunits of HVA channels, an $\alpha 2\delta$, a γ and four β subunits. Recent molecular cloning studies have identified a seventh $\alpha 1$ gene, which appears to encode a retinal-specific L-type channel, as well as two new genes for $\alpha 2\delta$ ($\alpha 2\delta$-2, $\alpha 2\delta$-3; [4]) and three for γ (γ-2 [5], γ-3 [6], γ-4 L. L. Cribbs and E. Perez-Reyes, unpublished observations). Mutations in many of these genes have been linked to human diseases and mouse models of epilepsy [5, 7, 8]. Since no combination of these subunits produced a T-type channel, efforts continued to clone additional members of the Ca^{2+} channel family.

Cloning of three members of the T-type Ca^{2+} channel family

Two excellent methods for cloning related genes are slow stringency hybridization and polymerase chain reaction (PCR). However, despite considerable effort these methods were not successful in cloning T-type channels. A new method for cloning genes is to search the GenBank, which contains all the known genes, plus many genomic and complementary DNA (cDNA) sequences. This in silico cloning or bioinformatic approach was used to clone the first member of the potassium channel family that contains two pore domains [9]. One way to screen the GenBank is to perform a homology search using the BLAST sequence align-

ment program [10], and search for genes that have a conserved motif, such as a pore loop. This approach led to the identification of two novel sequences from the *Caenorhabditis elegans* genome [11] that appeared to encode calcium channels (on cosmids C54d2 and C27f2) [12].

A different strategy is to search the GenBank using a text-based search. For example, many interesting sequences can be identified by searching for entries that contain the terms 'calcium', 'channel' and 'similar'. This led to the identification of the human clone H06096, which turned out to be a fragment of α1G [13]. This clone had been isolated by the LLNL Consortium as part of an effort to identify all messenger RNAs (mRNAs), or expressed sequence tagged (EST) genes [14]. The Consortium sequences a part of an EST, compares that to the known genes, submits the sequence to the GenBank along with a comment on which gene it is most similar to, then makes the clone available. Sequencing of H06096 (LLNL clone ID no. 44039; GenBank no. AF029228) strongly suggested that it was part of a novel Ca^{2+} channel gene. BLAST searches of the GenBank revealed that H06096 was related to the *C. elegans* sequence found on cosmid C54d2. It was then used to screen rat brain and human heart cDNA libraries, eventually isolating full-length cDNAs for both α1G, H and I [13, 15, 16]. Similar approaches have been used in a number of laboratories, leading to the cloning of the human α1H [17], mouse α1G [18], rat α1G [19], and human α1G and α1I [20]. The sequences of these three genes are homologous to the HVA channels, but clearly form a new subfamily (fig. 1). The other two subfamilies include the L-type family (α1S, C, D and F) and the non-L-type, HVA family (α1A, B and E). The *C. elegans* genome contains one representative of each subfamily, indicating that these genes evolved a long time ago.

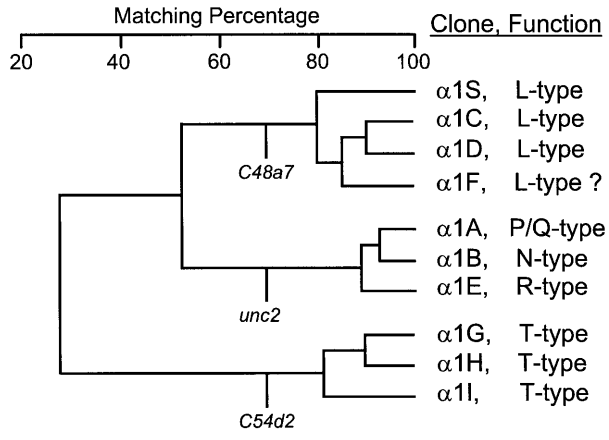

Figure 1. Dendrogram illustrating the Ca^{2+} channel subfamilies. The full-length sequence of each α1 subunit was first reduced to just the membrane-spanning regions, which produced a file containing 350 amino acids. These files were then aligned using WDNASIS software (Hitachi, San Bruno, CA, USA) based on the CLUSTAL algorithm [88]. Adapted from Lee et al. [21].

A mammalian homolog of the *C. elegans* C27f2 sequence was also cloned [21]. This cDNA encoded a protein that has considerable sequence identity to sodium and calcium channels. Unfortunately, it has not been possible to measure any channel activity from this clone in either oocytes or transfected HEK-293 cells [21].

Voltage-gated calcium channels are part of a superfamily that includes the highly related sodium channels and more distantly related potassium channels [22]. Due to this sequence identity, it is likely that their three-dimensional structures are also similar. Recently the structure of a potassium channel was solved by X-ray analysis [23]. This KcsA K^+ channel is composed of two transmembrane α helices separated by a pore loop (fig. 2). There are many K^+ channels that are predicted to have this structure, such as the family of inward rectifiers. Voltage-gated K^+ channels also contain highly similar sequences, but in addition they appear to have evolved four new transmembrane segments (S1–S4). Notably the S4 segment contains positively charged residues in every third position and acts as the voltage sensor that couples membrane depolarization to channel gating. Four of these α subunits are required to form a functional K^+ channel [24]. In contrast, voltage-gated calcium and sodium channels are much larger proteins that contain four of these repeats. It is likely that they arose from voltage-gated K^+ channels by two rounds of gene duplication [25]. Although the sequences of this ion channel superfamily can be aligned [22], the level of homology is in fact quite low. Many of the amino acid substitutions are conservative; hydrophobic residues such as leucine are often replaced by other hydrophobic residues such as isoleucine, valine or phenylalanine. Therefore, the hydropathy plot of a typical voltage-gated K^+ channel is nearly identical to one of the repeats of a Ca^{2+} channel (fig. 2A). Ion channels are often represented by snake diagrams (fig. 2B), where the protein is shown to snake its way through the membrane in a linear fashion, and the α helices are shown as boxes. This type of diagram overemphasizes the membrane-spanning regions. In fact, less than one-sixth of the protein is embedded in lipid. To illustrate this point each amino acid is represented with a circle (bottom right panel of fig. 2B). Clearly the bulk of the protein is in the cytoplasm, and the only significant portion that is predicted to be extracellular is the loop between the S5 segment and the pore loop in repeat I. In general, all voltage-gated Ca^{2+} and Na^+ channels

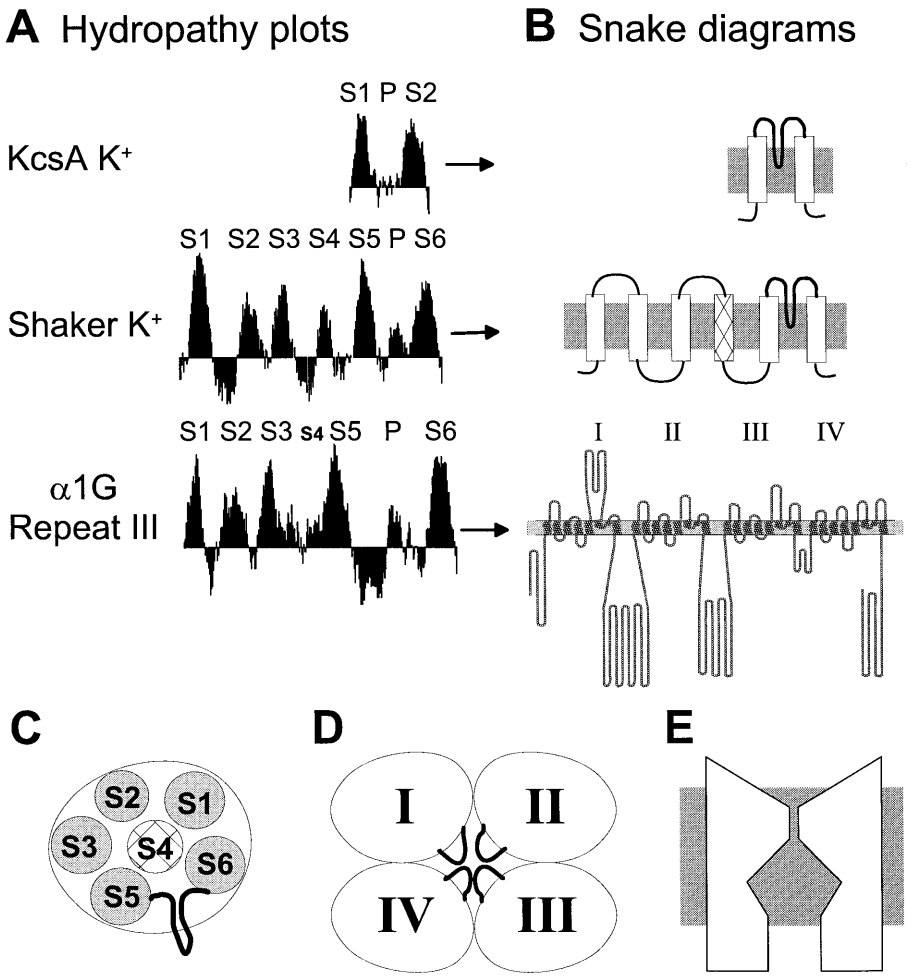

Figure 2. Predicted structure of ion channels. (*A*) Hydropathy plots of the KcsA and *Shaker* potassium channels, and repeat III of α1G. The hydropathy index varies 3 to -1. Letters above the plots indicate the relative position of each transmembrane segment (S1–S6) and pore loop (P). The S4 voltage sensors in most Ca^{2+} and Na^{+} channels are not very hydrophobic, so they are difficult to see in these plots. (*B*) Snake diagrams illustrating the transmembrane segments as though looking into the plane of the lipid bilayer (grey box). The S4 voltage sensor is hatched. The T-type channel (α1H) is illustrated with every amino acid replaced with a circle, and the relative position of each of the repeats is shown by the roman numerals. (*C*) Possible arrangement of the transmembrane segments in an individual repeat. This view is though looking down on the channel from outside the cell. (*D*) Arrangement of the four repeats with the pore loops shown to angle towards the center of the pore. (*E*) Stylized view of the channel from the side. The channel is shown in the open position. Closing of the channel may occur by closing of the internal channel walls.

are similar, with large linkers joining repeats I–II and II–III and much smaller III–IV linkers. The sequence of these linkers is poorly conserved. These linkers are used in HVA channels as a point of contact for a wide variety of regulatory proteins. For example, the I–II linker binds both the Ca^{2+} channel β and the G protein β subunit; the II–III linker of the skeletal muscle L-type channel interacts directly with the sarcoplasmic Ca^{2+} release channel, whereas this linker in α1A and B interacts with synaptic vesicle machinery; and the carboxy terminus has been implicated in Ca^{2+}-dependent inactivation of α1C channels (reviewed in [3]). Although the role of these linkers in T-type channels is unknown, one hypothesis is that they may serve as inactivation gates, as shown for the Na^{+} channel III–IV linker [26].

Models have been developed for the three-dimensional structure of voltage-gated Na^{+} channels [27, 28] and K^{+} channels [29], but not Ca^{2+} channels. The models of K^{+} channels have been meticulously updated with the reams of site-directed mutagenesis studies performed on cloned channels, and agree quite well with the solved structure. The S1–S3 segments are thought to form the outside of the channel, whereas the channel walls are lined by S5 and S6 segments (fig. 2C). The S4

segment lies in the center of the repeat in a gating pore. It is envisaged to slide up upon depolarization, leading to channel opening, then down upon repolarization to close the channels [29]. The movement of these charges produces the gating current that preceded the ionic current. The four repeats are arranged in a clockwise fashion (fig. 2D). This arrangement is predicted by studies on the dihydropyridine binding site, which includes amino acids in IIIS5, IIIS6 and IVS6 [30]. The pore loops are thought to project to the middle of the channel, forming a selectivity filter near the outer mouth of the channel (fig. 2E). The pore loops are particularly well conserved within an ion channel class, and even between each of the four repeats. Within each pore loop of HVA Ca^{2+} channels there is a glutamate residue located at the same position, leading to the shorthand notation EEEE. Site-directed mutagenesis of these glutamates has shown that they are the key determinants of a Ca^{2+} binding site that is crucial for selectivity [31–33]. In Na^{+} channels these residues are DEKA, and mutation of these residues to DEEE results in channels that are Ca^{2+}-permeable [34]. In T-type channels these residues are EEDD, indicating that the overall charge is conserved, but suggesting that binding of Ca^{2+} may be different. Indeed, studies on native T channels demonstrated that there were important differences in selectivity between LVA and HVA channels [35, 36].

Electrophysiological properties of the cloned T-type channels

Studies on native Ca^{2+} channels established the following criteria for distinguishing T-type channels from high voltage-activated channels such as N- and L-type: their activation at lower voltages (threshold of -70 vs. -40 mV), inactivation at lower voltages, their transient kinetics (inactivation τ of ~ 20 ms), which produces a distinctive pattern of criss-crossing traces during a current-voltage (I–V) protocol, slower deactivation leading to a prominent tail current after a depolarizing pulse, smaller single channel conductance in isotonic Ba^{2+} (~ 8 vs. 13–25 pS), similar conductance in Ca^{2+}, resistance to rundown, sensitivity to micromolar Ni^{2+} and insensitivity to various calcium channel blockers such as dihydropyridines and *Conus* toxins [37–42]. These criteria establish the properties that a cloned channel must fulfill to be called a T-type channel. Two common expression systems used to characterize cloned ion channels are *Xenopus laevis* oocytes and the mammalian cell line HEK-293. For oocyte experiments eggs are injected with 1–30 ng of in vitro synthesized complementary RNA (cRNA), then recorded currents 4–8 days later using the two-microelectrode voltage clamp. Using this system, the currents induced by injection of α1G were characterized [13]. It was demonstrated that α1G channels were activated at low voltages, inactivated rapidly producing criss-crossing kinetics, inactivated at negative potentials, had slow deactivation and a small single channel conductance in Ba^{2+}. These currents were compared with those produced by α1E, which had been proposed to be a member of the LVA family based on its inactivation at negative potentials and sensitivity to Ni^{2+} [43]. In contrast to α1G, α1E channels required much stronger depolarizations to open (30 mV) and inactivate (20 mV). Another major difference was the position of the reversal potential, which was 20 mV more positive for α1E, suggesting differences in permeability.

Initial attempts to express α1H in oocytes failed; however, large currents were readily obtained in transiently transfected HEK-293 cells [15]. It was demonstrated that α1H also produced channels that activated at low voltages, had criss-crossing kinetics, inactivated at negative potentials, had slow tail currents and a small single channel conductance in Ba^{2+} [15]. Addition of 5′ and 3′ untranslated sequences from *Xenopus* β-globin has allowed expression of α1H in oocytes [J.-H. Lee, L. L. Cribbs, E. Perez-Reyes, unpublished observations]. Therefore, as shown for K^{+} channels, these sequences can provide a big boost in expression [24]. The α1G currents have also been characterized in HEK-293 cells [16]. The currents carried by α1G and α1H appear to be nearly identical when recorded using Ba^{2+} as charge carrier in either expression system [16]. However, their kinetics differ when using Ca^{2+} as the charge carrier, with α1H activating and inactivating more slowly [44]. In contrast, expression of α1I produced a channel with drastically different kinetics (fig. 3A), especially when expressed in oocytes [16]. Since there were no reports of such a slowly activating LVA current, it was feared that there might be a mutation in the clone, as had occurred in the cloning of the rat II Na^{+} channel [45]. Therefore, the full-length construct was resequenced. No striking differences were found in the sequence of the rat α1I sequence when compared with either of the other cloned T channels, or with a partial human genomic sequence of α1I (GenBank no. AL008716). Surprisingly the α1I currents activated and inactivated five times faster in HEK-293 cells than observed in oocytes. These findings suggest that HEK-293 cells may express an auxiliary subunit of T channels that regulates kinetics. Support for this hypothesis comes from studies on HVA channels showing that β subunits can have a dramatic effect on kinetics [46] and the voltage-dependence of HVA channel gating [47]. However, the putative LVA subunit appears not to affect the voltage dependence, since the I–V curves obtained in oocytes were nearly identical to those obtained in HEK-293 cells [16]. Preliminary re-

sults suggest that the known β subunits do little to α1G currents, whereas coexpression with $\alpha 2\delta$ leads to an increased number of channels at the surface membrane in COS cells [48], but not in HEK-293 cells [49]. Despite the slowness of the kinetics, α1I currents still display the classic criss-crossing pattern during an I–V protocol. They also activate and inactivate over a similar voltage range as native T-type currents. The single channel conductance (11 pS) was significantly larger than that observed with α1G or H (5–7 pS), and approaches the value obtained for α1E [50]. There was also a prominent subconductance state (4 pS), as had been observed previously for native T-type channels [51, 52]. Stably transfected cell lines of α1G, H and I have been generated, which allowed comparative studies of their biophysical properties using either 10 mM Ba^{2+} as charge carrier [16] (fig. 3) or more physiologically relevant solutions containing 1.25 mM Ca^{2+} [44]. All three channels activated and inactivated over a similar range, and plots of the activation curve and the steady-state inactivation (5 s prepulse) curves indicated the existence of a window current (fig. 3C). The window current is a range where channels can activate, but never fully inactivate. These window currents occurred near the resting membrane potential of many cells, suggesting that T-type channels can play a role in maintaining basal concentrations of Ca^{2+}.

Tissue localization of α1G, H and I

Northern blot analysis of human mRNA indicates that α1G, H and I are all abundantly expressed in brain [13, 15, 16]. Heart expresses both α1G and H. We also detected abundant expression of α1H in kidney. Similar results were obtained for α1H expression by Williams et al. [17], except they also detected cross-reactive material

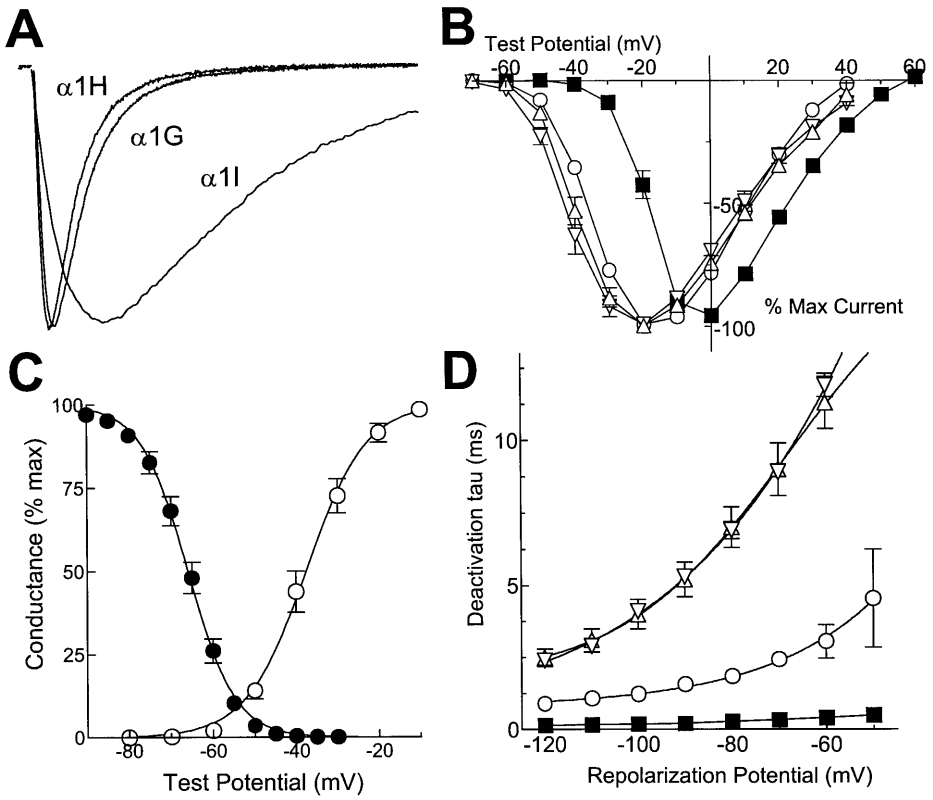

Figure 3. Electrophysiological recordings of cloned T-type Ca^{2+} channels. (*A*) Traces obtained during pulses to -20 mV for HEK-293 cells transfected with either α1G, H or I. The first 100 ms of the traces are shown. The currents have been scaled, but were roughly 1 nA at peak. (*B*) Normalized current-voltage relationships for α1G (triangles), α1H (inverted triangles), α1I (circles) and α1E (squares). The data from individual cells was normalized to the peak current for that cell, then averaged. Alternatively, activation curves can be represented by transforming the data to conductance using the constant field equation. (*C*) The inactivation of α1I channels was determined using 5-s prepulses, then plotted with the activation curve. The overlap region centered at -55 mV represents the window current region. Data were obtained with 10 mM Ba^{2+} as charge carrier at room temperature. (*D*) Deactivation kinetics of all four channels (same symbols as in *B*). Adapted from Lee et al. [16].

Table 1. Distribution of α1G H and I mRNA in the rat brain.

Brain region	α1G	α1H	α1I	Brain region	α1G	α1H	α1I
Olfactory system				Thalamus			
olf. bulb glomerular	+	bt	+++	principal rely nuc.	+++	bt	+
olf. bulb granule cells	++++	++++	++++	intralaminar	+++++	bt	+
Islands of Callega	+	+++++	+++++	geniculate	++	bt	+
Basal forebrain				reticular	bt	++	+++
striatum	bt	++	++	lateral habenula	+++	bt	+++
globus pallidus	bt	bt	bt	Midbrain and pons			
subthalamic nucleus	++	+	+++	periaqueductal g	++	+	bt
bed nuc. stria term.	+++++	++	+	tegmental nuclei	+++	bt	+
claustrum	+++++	bt	+	raphe	+	+	bt
Amygdala	++/+++	+/++		substantia nigra	+	+	bt
Cerebral cortex				Cerebellum and olive			
layers II/III	++	bt/+	+	granule-anterior	+	bt	++
layers IV	+++	bt	++	granule-posterior	++++	bt	++
layers V	++	++	+	Purkinje	+++++	bt	bt
layers Vl	+++	bt	+	molecular	+	bt	bt
piriform cortex	+++	+++	+++/bt	deep cerebellar n.	+	bt	bt
Hippocampus				inferior olive	+++++	bt	++
pyramidals (CA1–3)	++/+++	+++/+++++	++/+++++	Other			
granule cells of DG	++	+++++	+	sup. cerv. gang.	+	bt	bt
polymorph of DG	++	++	++	pineal gland	+	++++	bt
Hypothalamus	++/+++	+/++	+	pituitary	+	+++	+
Medulla and spinal cord	bt/+++	bt/+	bt/+	sensory ganglia	+	++++	++

Adapted from Talley et al. (1999). +++++, highest levels of labeling; ++++, very high, +++, high; ++, moderate; +, low; bt, below threshold detection.

in pancreas, skeletal muscle, lung and placenta. Perhaps this distribution in peripheral tissues is due to expression of α1H in smooth muscle. Transcripts of α1I were only detected in brain [16], where they have a wide distribution (table 1). The distribution of these mRNAs in rat brain has also been examined in detail [53]. The probes were 33-bp oligonucleotides based on sequence of the I–II loop, which is poorly conserved among the three genes, reducing the possibility of cross-reactivity. Somewhat surprisingly, there was evidence for T-channel expression throughout the brain. For example, messages for all three channels could be detected in all the layers of the cerebral cortex, not just layer V as suggested from electrophysiological recordings [54]. Other brain regions that expressed message for all three channels included the olfactory bulb and hippocampus (table 1). Many brain regions expressed only two T channels. However, α1G was rarely expressed with α1H alone; rather, they both took turns expressing with α1I. For example, α1G and I were coexpressed in the cerebellum, lateral habenula and inferior olive, whereas α1H and I were coexpressed in the striatum and the thalamic reticular nucleus. Interestingly, currents that inactivate as slowly as α1I have been recorded from neurons isolated from the lateral habenula, thalamus and reticular nucleus [55–57].

Although antibodies for all three channels have not been developed, there have been antibodies raised against the I–II loop of α1G. This antibody was used to map the distribution of the α1G protein in rat brain [58]. In general there was good agreement between the mRNA and protein distribution, although there were a few regions where there was either a stronger or weaker signal than expected from the message levels. Immunoreactivity was detected on both the soma and dendrites. Strong immunoreactivity was detected in the following brain regions: cerebellum, hypoglossal and trigeminal nuclei, inferior olive, lateral, medullary and rostroventrolateral reticular nuclei, nucleus prepositus, external cuneate nucleus, raphe nuclei, inferior colliculus and throughout the cerebral cortex.

Possible physiological roles of T-type channels

One of the first physiological roles proposed for low voltage-activated channels was as a pacemaker current.

Ca^{2+} entry itself leads to depolarization of the membrane, which can then activate other voltage-gated channels. However, the membrane must be depolarized by some other ionic current before T channels can open; therefore they are just one of many pacemaker currents. A similar pacemaker role was demonstrated for T-type channels in the heart [59]. Inhibition of the T-type current with $NiCl_2$ slowed the late phase of diastolic depolarization, resulting in a negative chronotropic effect [59–61]. The early phase of diastolic depolarization is mediated by the current called I_f (reviewed in [62]). In higher mammals such as rats, dogs and cats, low voltage-activated currents have been found in atrial myocytes, sino-atrial nodal cells, latent atrial pacemaker cells and in Purkinje fibers [59, 60, 63, 64]. In these mammals only L-type currents are detected in adult ventricular myocytes (reviewed in [42]); however, T-type currents have been recorded in myocytes isolated from a pressure-overload model of cardiac hypertrophy [65].

A similar pacemaker role has been described in neurons, where T-type channels produce the low threshold Ca^{2+} spike that is crowned by a burst of Na^+-dependent action potentials [66–72]. Thalamic neurons alternate between at least two modes of activity, burst and tonic firing, which correlate with their resting membrane potential. During tonic firing the membrane is depolarized to around -50 mV, and action potentials are triggered by Na^+ channels. Burst firing occurs when the membrane potential is depolarized from a typical resting membrane potential (below -70 mV), and is due to the sequential activation of T-type Ca^{2+} and Na^+ channels. The trigger for this activity can be a small excitatory postsynaptic potential (EPSP). If the resting membrane potential is in the range where T-type channels can activate, then burst firing can be triggered by *inhibitory* postsynaptic potentials (IPSPs). This is due to the ability of T-type channels to recover from inactivation during the IPSP, then fire as the IPSP wears off. This type of neuronal firing was originally termed postanodal exaltation in the 50s (see references cited in [73]) and is now referred to as rebound burst firing. When the inhibitory interneuron is interconnected with the neuron that contains T channels, then this circuit is capable of generating stable oscillations and resonance. Such circuits have been well described for the corticothalamic loop (reviewed in [74]). These oscillations are usually only observed during sleep, producing a spike-wave or sleep spindle in the electroencephalogram (EEG). Similar EEG patterns are observed during absence epileptic seizures [75, 76], and in some animal models of epilepsy [77]. The ability of antiepileptic drugs to block T-type channels in vitro led to the hypothesis that some forms of epilepsy may be caused by overactive T-type channels [78], but see [79]. This hypothesis is supported by the finding of increased T-channel activity in a rat model of absence epilepsy [80].

The slow deactivation kinetics of T-type channels (fig. 3D) should allow for large fluxes of Ca^{2+} during the repolarization phase of an action potential. This could lead directly to an afterdepolarizing potential [72], or it could couple to Ca^{2+}-dependent K^+ channels, producing afterhyperpolarizations [66]. Evidence for this coupling was provided by studies where T-type channels were blocked either pharmacologically [81] or with antisense depletion [82].

Due to their activation so close to the resting membrane potential of most cells, and the existence of a window current, T-type channels can also play a role in maintaining intracellular Ca^{2+} concentrations. This may be particularly important in nonexcitable cells, or cells that have slowly developing depolarizations. Hormone secretions from both adrenal glomerulosa and fasciculata cells have been shown to rely on T-type Ca^{2+} channels [83, 84]. T-type currents have been detected in a wide variety of secretory cells and smooth muscle myocytes [42]. Smooth muscle myocytes also express L-type currents. Block of smooth muscle L-type Ca^{2+} channels leads to a lowering of blood pressure, and is the proposed mechanism of action of many clinically relevant drugs. Mibefradil was a novel antihypertensive drug that blocked T-type channels at clinically relevant concentrations (0.2 μM), whereas block of L-type channels occurred at 15-fold higher concentrations [42]. These results suggested that T-type channels may play an important role in setting vascular tone. Another interesting property of mibefradil was its ability to block smooth muscle proliferation [85]. T-type channel expression is tightly coupled to the cell cycle [86]. These results suggest that Ca^{2+} influx through T-type channels may be an important determinant of cell proliferation, and that selective T-type antagonists may be useful in preventing restenosis after balloon angioplasty. Unfortunately mibefradil was withdrawn from the market due to its inhibition of cytochrome P-450, which is a key enzyme in the metabolism of many drugs [87]. In conclusion, mibefradil provides support for the concept that block of T-type channels will be clinically useful. Cloning and expression of these channels provides an assay for the development of new classes of calcium channel blockers.

Acknowledgements. I would like to thank Leanne Cribbs, Jung-Ha Lee, Asif Daud and Qun Jiang for the dedication and hard work which made these studies possible. This work was supported by a grant from the National, Heart, Lung and Blood Institute, no. HL57828.

1 Perez-Reyes E. and Schneider T. (1995) Molecular biology of calcium channels. Kidney Int. **48:** 1111–1124
2 Hofmann F., Biel M. and Flockerzi V. (1994) Molecular basis for Ca^{2+} channel diversity. Annu. Rev. Neurosci. **17:** 399–418
3 Walker D. and De Waard M. (1998) Subunit interaction sites in voltage-dependent Ca^{2+} channels: role in channel function. Trends Neurosci. **21:** 148–154
4 Klugbauer N., Lacinova L., Marais E., Hobom M. and Hofmann F. (1999) Molecular diversity of the calcium channel alpha2delta subunit. J. Neurosci. **19:** 684–691
5 Letts V. A., Felix R., Biddlecome G. H., Arikkath J., Mahaffey C. L., Valenzuela A. et al. (1998) The mouse stargazer gene encodes a neuronal Ca^{2+}-channel γ subunit. Nature Genet. **19:** 340–347
6 Black J. L., III and Lennon V. A. (1999) Identification and cloning of putative human neuronal voltage-gated calcium channel gamma-2 and gamma-3 subunits: neurologic implications. Mayo Clin. Proc. **74:** 357–361
7 Ophoff R. A., Terwindt G. M., Frants R. R. and Ferrari M. (1998) P/Q-type Ca^{2+} channel defects in migraine, ataxia and epilepsy. Trends Pharmacol. Sci. **19:** 121–127
8 Burgess D. L., Jones J. M., Meisler M. H. and Noebels J. L. (1997) Mutation of the Ca^{2+} channel subunit gene *Cchb4* is associated with ataxia and seizures in the lethargic (*lh*) mouse. Cell **88:** 385–392
9 Ketchum K. A., Joiner W. J., Sellers A. J., Kaczmarek L. K. and Goldstein S. A. N. (1996) A new family of outwardly rectifying potassium channel proteins with two pore domains in tandem. Nature **376:** 690–695
10 Altschul S. F., Gish W., Miller W., Myers E. W. and Lipman D. J. (1990) Basic local alignment search tool. J. Mol. Biol. **215:** 403–410
11 Anonymous (1998) Genome sequence of the nematode *C. elegans*: a platform for investigating biology. Science **282:** 2012–2018
12 Perez-Reyes E., Lee J.-H., Daud A. and Cribbs L. L. (1997) Cloning of calcium channels representing two new subfamilies distinct from high voltage-activated types Biophys. J. **72:** A146
13 Perez-Reyes E., Cribbs L. L., Daud A., Lacerda A. E., Barclay J., Williamson M. P. et al. (1998) Molecular characterization of a neuronal low voltage-activated T-type calcium channel. Nature **391:** 896–900
14 Lennon G., Auffray C., Polymeropoulus M. and Soares M. B. (1996) The I.M.A.G.E. Consortium: an integrated molecular analysis of genomes and their expression. Genomics **33:** 151–152
15 Cribbs L. L., Lee J.-H., Yang J., Satin J., Zhang Y., Daud A. et al. (1998) Cloning and characterization of α1H from human heart, a member of the T-type calcium channel gene family. Circ. Res. **83:** 103–109
16 Lee J.-H., Daud A. N., Cribbs L. L., Lacerda A. E., Pereverzev A., Klockner U. et al. (1999) Cloning and expression of a novel member of the low voltage-activated T-type calcium channel family. J. Neurosci. **19:** 1912–1921
17 Williams M. E., Washburn M. S., Hans M., Urrutia A., Brust P. F., Prodanovich P. et al. (1999) Structure and functional characterization of a novel human low-voltage activated calcium channel. J. Neurochem. **72:** 791–799
18 Klugbauer N., Marais E., Lacinova L. and Hofmann F. (1999) A T-type calcium channel from mouse brain. Pflugers Arch. **437:** 710–715
19 Zhuang H., Hu F., Bhattacharjee A., Zhang M., Wu S., Berggren P.-O. et al. (1999) Cloning of the rat β-cell T-type caclium channel α1 subunit and its regulation by glucose. Biophys. J. **76:** A409
20 Monteil A., Chemin J., Mennessier G., Berta P., Bourinet E., Nargeot J. et al. (1999) Cloning and molecular characterization of α1G and α1I isoforms of human T-type Ca^{2+} channels. Biophys. J. **76:** A408
21 Lee J.-H., Cribbs L. L. and Perez-Reyes E. (1999) Cloning of a putative four repeat ion channel from rat brain. FEBS Lett. **445:** 231–236
22 Jan L. Y. and Jan Y. N. (1990) A superfamily of ion channels. Nature **345:** 672
23 Doyle D. A., Cabral J. M., Pfuetzner R. A., Kuo A., Gulbis J. M., Cohen S. L. et al. (1998) The structure of the potassium channel: molecular basis of K^+ conduction and selectivity. Science **280:** 69–77
24 Liman E. R., Tytgat J. and Hess P. (1992) Subunit -stoichiometry of a mammalian K+ channel determined by construction of multimeric cDNAs. Neuron **9:** 861–871
25 Strong M., Chandy K. G. and Gutman G. A. (1993) Molecular evolution of voltage-sensitive ion channel genes: on the origins of electrical excitability. Mol. Biol. Evol. **10:** 221–242
26 Miller A. and Hu B. (1995) A molecular model of low-voltage-activated calcium conductance. J. Neurophysiol. **73:** 2349–2356
27 Greenblatt R. E., Blatt Y. and Montal M. (1985) The structure of the voltage-sensitive sodium channel. Inferences derived from computer-aided analysis of the *Electrophorus electricus* channel primary structure. FEBS Lett. **193:** 125–134
28 Guy H. R. and Seetharamulu P. (1986) Molecular model of the action potential sodium channel. Proc. Natl. Acad. Sci. USA **83:** 508–512
29 Durell S. R., Hao Y. and Guy H. R. (1998) Structural models of the transmembrane region of voltage-gated and other K^+ channels in open, closed, and inactivated conformations. J. Struct. Biol. **121:** 263–284
30 Mitterdorfer J., Grabner M., Kraus R., Hering S., Prinz H., Glossmann H. et al. (1998) Molecular basis of drug interaction with L-type Ca^{2+} channels. J. Bioenerg. Biomembr. **30:** 319–334
31 Yang J., Ellinor P. T., Sather W. A., Zhang J. F. and Tsien R. W. (1993) Molecular determinants of Ca^{2+} selectivity and ion permeation in L-type Ca^{2+} channels. Nature **366:** 158–161
32 Tang S., Mikala G., Bahinski A., Yatani A., Varadi G. and Schwartz A. (1993) Molecular localization of ion selectivity sites within the pore of a human L-type cardiac calcium channel. J. Biol. Chem. **268:** 13026–13029
33 Parent L. and Gopalakrishnan M. (1995) Glutamate substitution in Repeat IV alters divalent and monovalent cation permeation in the heart Ca^{2+} channel. Biophys. J. **69:** 1801–1813
34 Heinemann S. H., Terlau H., Stuhmer W., Imoto K. and Numa S. (1992) Calcium channel characteristics conferred on the sodium channel by single mutations. Nature **356:** 441–443
35 Carbone E. and Lux H. D. (1987) Kinetics and selectivity of a low-voltage-activated calcium current in chick and rat sensory neurones. J. Physiol. **386:** 547–570
36 Shuba Y. M., Teslenko V. I., Savchenko A. N. and Pogorelaya N. H. (1991) The effect of permeant ions on single calcium channel activation in mouse neuroblastoma cells: ion-channel interactions. J. Physiol. **443:** 25–44
37 Carbone E. and Lux H. D. (1984) A low voltage-activated, fully inactivating Ca channel in vertebrate sensory neurones. Nature **310:** 501–502
38 Nilius B., Hess P., Lansman J. B. and Tsien R. W. (1985) A novel type of cardiac calcium channel in ventricular cells. Nature **316:** 443–446
39 Matteson D. R. and Armstrong C. M. (1986) Properties of two types of calcium channels in clonal pituitary cells. J. Gen. Physiol. **87:** 161–182
40 Tsien R. W., Lipscombe D., Madison D. V., Bley K. R. and Fox A. P. (1988) Multiple types of neuronal calcium channels and their selective modulation. Trends Neurosci. **11:** 431–438
41 Randall A. D. and Tsien R. W. (1997) Contrasting biophysical and pharmacological properties of T- type and R-type calcium channels. Neuropharmacol. **36:** 879–893
42 Ertel S. I., Ertel E. A. and Clozel J. P. (1997) T-type Ca^{2+} channels and pharmacological blockade: potential pathophysiological relevance. Cardiovasc. Drugs Ther. **11:** 723–739
43 Soong T. W., Stea A., Hodson C. D., Dubel S. J., Vincent S. R. and Snutch T. P. (1993) Structure and functional expres-

sion of a member of the low voltage-activated calcium channel family. Science **260:** 1133–1136
44 Klockner U., Lee J. H., Cribbs L. L., Daud A., Hescheler J., Pereverzev A. et al. Comparison of the Ca^{2+} currents induced by expression of three cloned $\alpha 1$ subunits, $\alpha 1G$, $\alpha 1H$, and $\alpha 1I$, of low voltage-activated T-type Ca^{2+} channels. Eur. J. Neurosci., (in press)
45 Auld V. J., Goldin A. L., Krafte D. S., Catterall W. A., Lester H. A., Davidson N. et al. (1990) A neutral amino acid change in segment IIS4 dramatically alters the gating properties of the voltage-dependent sodium channel. Proc. Natl. Acad. Sci. USA **87:** 323–327
46 Lacerda A. E., Kim H. S., Ruth P., Perez-Reyes E., Flockerzi V., Hofmann F. et al. (1991) Normalization of current kinetics by interaction between the alpha1 and beta subunits of the skeletal muscle dihydropyridine-sensitive Ca^{2+} channel. Nature **352:** 527–530
47 Perez-Reyes E., Castellano A., Kim H. S., Bertrand P., Baggstrom E., Lacerda A. E. et al. (1992) Cloning and expression of a cardiac/brain beta subunit of the L-type calcium channel. J. Biol. Chem. **267:** 1792–1797
48 Dolphin A. C., Wyatt C. N., Richards J., Beattie R. E., Craig P., Lee J.-H. et al. (1999) The effect of $\alpha 2$-δ and other accessory subunits on expression and properties of the calcium channel $\alpha 1G$. J. Physiol. **519:** 35–45
49 Lacinova L., Klugbauer N. and Hofmann F. (1999) Absence of modulation of the expressed caclium channel (1G subunit by $\alpha 2\delta$ subunits. J. Physiol **516.3:** 639–645
50 Bourinet E., Zamponi G. W., Stea A., Soong T. W., Lewis B. A., Jones L. P. et al. (1996) The α_{1E} calcium channel exhibits permeation properties similar to low-voltage-activated calcium channels. J. Neurosci. **16:** 4983–4993
51 Carbone E. and Lux H. D. (1987) Single low-voltage-activated calcium channels in chick and rat sensory neurones. J. Physiol. **386:** 571–601
52 Droogmans G. and Nilius B. (1989) Kinetic properties of the cardiac T-type calcium channel in the guinea-pig. J. Physiol. **419:** 627–650
53 Talley E. M., Cribbs L. L., Lee J.-H., Daud A., Perez-Reyes E. and Bayliss D. (1999) Differential distribution of three members of a gene family encoding low voltage-activated (T-type) calcium channels. J. Neurosci. **19:** 1895–1911
54 de la Pena E. and Geijo-Barrientos E. (1996) Laminar localization, morphology and physiological properties of pyramidal neurons that have the low-threshold calcium current in the guinea-pig medial frontal cortex. J. Neurosci. **16:** 5301–5311
55 Huguenard J. R., Gutnick M. J. and Prince D. A. (1993) Transient Ca^{2+} currents in neurons isolated from rat lateral habenula. J. Neurophysiol. **70:** 158–166
56 Tarasenko A. N., Kostyuk P. G., Eremin A. V. and Isaev D. S. (1997) Two types of low-voltage-activated Ca^{2+} channels in neurones of rat laterodorsal thalamic nucleus. J. Physiol. **499:** 77–86
57 Huguenard J. R. and Prince D. A. (1992) A novel T-type current underlies prolonged Ca(2 +)-dependent burst firing in GABAergic neurons of rat thalamic reticular nucleus. J. Neurosci. **12:** 3804–3817
58 Craig P. J., Beattie R. E., Folly E. A., Banerjee M. D., Reeves M. B., Priestley J. V. et al. (1999) The expression of the voltage-dependent calcium channel $\alpha 1G$ subunit throughout the mature rat brain and its correlation with T-type currents. Eur. J. Neurosci. **11:** 2949–2964
59 Hagiwara N., Irisawa H. and Kameyama M. (1988) Contribution of two types of calcium currents to the pacemaker potentials of rabbit sino-atrial node cells. J. Physiol. **395:** 233–253
60 Zhou Z. and Lipsius S. L. (1994) T-type calcium current in latent pacemaker cells isolated from cat right atrium. J. Mol. Cell. Card. **26:** 1211–1219
61 Satoh H. (1995) Role of T-type Ca^{2+} channel inhibitors in the pacemaker depolarization in rabbit sino-atrial nodal cells. Gen. Pharmacol. **26:** 581–587
62 Campbell D. C., Rasmusson R. L. and Strauss H. C. (1992) Ionic current mechanisms generating vertebrate primary cardiac pacemaker activity at the single cell level: an integrative view. Annu. Rev. Physiol. **54:** 279–302
63 Hirano Y., Fozzard H. A. and January C. T. (1989) Characteristics of L- and T-type Ca^{2+} currents in canine cardiac Purkinje cells. Am. J. Physiol. **256:** H1478–1492
64 Tseng G.-N. and Boyden P. A. (1989) Multiple types of Ca^{2+} currents in single canine Purkinje cells. Circ. Res. **65:** 1735–1750
65 Nuss H. B. and Houser S. R. (1993) T-type Ca^{2+} current is expressed in hypertrophied adult feline left ventricular myocytes. Circ. Res. **73:** 777–782
66 Llinas R. and Yarom Y. (1981) Properties and distribution of ionic conductances generating electroresponsiveness of mammalian inferior olivary neurones in vitro. J. Physiol. **315:** 569–584
67 Llinas R. and Yarom Y. (1981) Electrophysiology of mammalian inferior olivary neurones in vitro. Different types of voltage-dependent ionic conductances. J. Physiol. **315:** 549–567
68 Llinas R. and Jahnsen H. (1982) Electrophysiology of mammalian thalamic neurons in vitro. Nature **297:** 406–408
69 Crunelli V., Lightowler S. and Pollard C. E. (1989) A T-type Ca^{2+} current underlies low-threshold Ca^{2+} potentials in cells of the cat and rat lateral geniculate nucleus. J. Physiol. **413:** 543–561
70 Suzuki S. and Rogawski M. A. (1989) T-type calcium channels mediate the transition between tonic and phasic firing in thalamic neurons. Proc. Nat. Acad. Sci. U.S.A. **86:** 7228–7232
71 Hernandez-Cruz A. and Pape H.-C. (1989) Identification of two calcium currents in acutely dissociated neurons form the rat lateral geniculate nucleus. J. Neurophysiol. **61:** 1270–1283
72 White G., Lovinger D. M. and Weight F. F. (1989) Transient low-threshold Ca^{2+} current triggers burst firing through an afterdepolarizing potential in an adult mammalian neuron. Proc. Natl. Acad. Sci. USA **86:** 6802–6806
73 Andersen P., Eccles J. C. and Sears T. A. (1964) The ventrobasal complex of the thalamus: types of cells, their responses and functional organization. J. Physiol. **174:** 370–399
74 McCormick D. A. and Bal T. (1997) Sleep and arousal: thalamocortical mechanisms. Annu. Rev. Neurosci. **20:** 185–215
75 Gloor P. and Fariello R. G. (1988) Generalized epilepsy: some of its cellular mechanisms differ from those of focal epilesy. Trends Neurosci. **11:** 63–68
76 Steriade M., Contreras D. and Amzica F. (1994) Synchronized sleep oscillations and their paroxysmal developments. Trends Neurosci. **17:** 199–208
77 Noebels J. L. (1994) Genetic and phenotypic heterogeneity of inherited spike-and-wave epilepsies. In: Idiopathic Generalized Epilepsies: Clinical, Experimental and Genetic Aspects, pp. 215–225, Malafosse A., Genton P., Hirsch E., Marescaux D., Broglin D. and Bernasconi R., (eds), John Libbey, London
78 Coulter D. A., Huguenard J. R. and Prince D. A. (1990) Differential effects of petit mal anticonvulsants and convulsants on thalamic neurones: calcium current reduction. Br. J. Pharmacol. **100:** 800–806
79 Leresche N., Parri H. R., Erdemli G., Guyon A., Turner J. P., Williams S. R. et al. (1998) On the action of the anti-absence drug ethosuxamide in the rat and cat thalamus. J. Neurosci. **18:** 4842–4853
80 Tsakiridou E., Bertollini L., de Curtis M., Avanzini G. and Pape H. C. (1995) Selective increase in T-type calcium conductance of reticular thalamic neurons in a rat model of absence epilepsy. J. Neurosci. **15:** 3110–3117
81 McCobb D. P. and Beam K. G. (1991) Action potential waveform voltage-clamp commands reveal striking differences in calcium entry via low and high voltage-activated calcium channels. Neuron **7:** 119–127

82 Lambert R. C., McKenna F., Maulet Y., Talley E. M., Bayliss D., Cribbs L. L. et al. (1998) Low voltage-activated Ca^{2+} currents are generated by members of the Ca_vT subunit family (α1G/H) in rat primary sensory neurons. J. Neurosci. **18:** 8605–8613

83 Cohen C. J., McCarthy R. T., Barrett P. Q. and Rasmussen H. (1988) Ca channels in adrenal glomerulosa cells: K + and angiotensin II increase T-type Ca channel current. Proc. Natl. Acad. Sci. USA **85:** 2412–2416

84 Enyeart J. J., Mlinar B. and Enyeart J. A. (1993) T-type Ca^{2+} channels are required for adrenocorticotropin-stimulated cortisol production by bovine adrenal zona fasciculata cells. Mol. Endocrinol. **7:** 1031–1040

85 Schmitt R., Clozel J. P., Iberg N. and Buhler F. R. (1996) Prevention of neointima formation by mibefradil after vascular injury in rats: comparison with ACE inhibition. Cardiovasc. Drugs and Ther. **10:** 101–105

86 Kuga T., Kobayashi S., Hirakawa Y., Kanaide H. and Takeshita A. (1996) Cell cycle-dependent expression of L- and T-type Ca^{2+} currents in rat aortic smooth muscle cells in primary culture. Circ. Res. **79:** 14–19

87 Welker H. A., Wiltshire H. and Bullingham R. (1998) Clinical pharmacokinetics of mibefradil. Clin. Pharmacokinet. **35:** 405–423

88 Higgins D. G. and Sharp P. M. (1988) CLUSTAL: a package for performing multiple sequence alignments on a microcomputer. Gene **73:** 237–244

.